Solid Earth Discuss., 6, 3333–3359, 2014
www.solid-earth-discuss.net/6/3333/2014/
doi:10.5194/sed-6-3333-2014

Solid Earth
Discussions
Open Access

Evaluation of soil fertility in the succession of karst rocky desertification using principal component analysis

L. W. Xie[1], J. Zhong[1], F. X. Cao[2], J. J. Li[1], and L. C. Wu[1]

[1]Key Laboratory of Cultivation and Protection for Non-Wood Forest Trees, Ministry of Education, Central South University of Forestry and Technology, Changsha 410004, Hunan, China
[2]College of Life Science and Technology, Central South University of Forestry and Technology, Changsha 410004, China

Received: 10 November 2014 – Accepted: 16 November 2014
– Published: 18 December 2014

Correspondence to: L. Wu (wulichao@sina.com)

Published by Copernicus Publications on behalf of the European Geosciences Union.

Abstract

Expanding of karst rocky desertification (RD) area in southwestern China has led to destructed ecosystem and local economic development lagging behind. It is important to understand the soil fertility at RD regions for the sustainable management of karst lands. The effects of the succession of RD on soil fertility were studied by investigating the stands and analyzing the soil samples with different RD grades in the central Hunan province, China, using the principal component analysis method. The results showed that the succession of RD had different impacts on soil fertility indicators. The changing trend of total organic carbon (TOC), total nitrogen (TN), available phosphorous (AP), microbial biomass carbon (MBC), and microbial biomass nitrogen (MBN) out of 19 selected indicators in different RD regions was: potential RD (PRD) > light RD (LRD) > moderate RD (MRD) > intensive RD (IRD), whereas the changing trend of other indicators was not entirely consistent with the succession of RD. The degradation trend of soil fertility was basically parallel to the aggravation of RD, and the strength of integrated soil fertility was in the order of PRD > MRD > LRD > IRD. The TOC, total phosphorus (TP), cation exchange capacity (CEC), MBC, MBN, microbial mass phosphorous (MBP), and bulk density (BD) could be regarded as the key indicators to evaluate the soil fertility due to their close correlations to the integrated fertility.

1 Introduction

Karst rocky desertification is a process of karst land degradation involving serious soil erosion, extensive exposure of bedrocks, and the appearance of a desert-like landscape, leading to drastic decrease in soil productivity (Wang et al., 2004b), and is recognized as an obstacle to local sustainable development (Wu et al., 2011). Some mountain areas of central Hunan province, China, being karst region covered with evergreen broad-leaved forest historically but now under deforestation and over-reclamation, are included in the largest karst geomorphologic distributing areas in southwestern China (Huang and Cai, 2007; Xiong et al., 2009). Climate changes and anthropogenic driving forces are responsible for the development of aeolian/sandy desertification (T. Wang et al., 2013; X. Wang et al., 2013) which can cause dust storms (Wang and Jia, 2013), soil and water losses (Cerdà and Lavée, 1999), and are also playing important roles in the aggravation of karst rocky desertification (Y. B. Li et al., 2009b; Yan and Cai, 2013). This has gradually attracted the national-wide attention in China, and the government and researchers are taking active measures to meliorate rocky desertification land by sustainable management (Bai et al., 2013; Huang et al., 2008).

For example, to enforce the sustainable management of karst lands, in 2011, a *Monitoring Rules of Rocky Desertification in Hunan Province* had been issued by Hunan Provincial Bureau of Forestry, in which rocky desertification (RD) was classified into 4 grades, namely potential RD (PRD), light RD (LRD), moderate RD (MRD), and intensive RD (IRD) based on the soil depth, vegetation coverage, vegetation type and bedrock exposure according to some reported classification methods (Wang et al., 2004a; Xiong et al., 2009) with minor modifications. The changing process of karst land from one grade to another was called succession of RD here and elsewhere (Xie and Wang, 2006), which means an observable process of changes of karst ecosystem such as vegetation type, vegetation coverage, bedrock exposure, and soil depth from PRD to IRD orderly or vice versa. Furthermore, on stands investigation, we found that some karst regions with higher grades (MRD or IRD) had been enclosed for afforestation. These measures are beneficial to rehabilitation and sustainable management of karst lands.

In the process of sustainable management, it is important to determine the status of soil quality on karst regions (Deng and Jiang, 2011; Li et al., 2013), because the soil quality is of fundamental importance for agricultural production and soil fertility management (irrigation, fertilization, and cultivation) (Fallahzade and Hajabbasi, 2012), and it is also a central issue in the decisions on food security, poverty reduction and environment management (Tilman et al., 2002). Soil fertility is a major component of soil quality, so investigation on soil fertility could be regarded as an essential prerequisite to rationally management and utilization of karst lands. However, soil fertility changes associated with the succession of RD in the karst lands have been poorly understood (Wang and Li, 2007) due to lacking of method how to evaluate the soil on areas affected by RD. Especially, using a minimum dataset to reduce the need for determining a broad range of indicators to assess soil fertility (Yao et al., 2013) of karst lands during succession of RD have not been achieved at present.

The soil fertility depends on local climate, soil-forming conditions, eco-environment, and anthropogenic influence in different regions (Liu et al., 2006). Choosing appropriate indicators is vital to evaluate soil fertility. Those indicators that influence plant growth should be included into evaluating system. Generally, evaluating indicators are chosen empirically based on the researching fruits of predecessors. But the adaptability of soil fertility indicators should be paid close attention to karst area due to its fragile ecosystem (Fu et al., 2010). Based on the analyses of literatures and suggestions from experts on the stands investigation, we evaluated soil fertility of karst lands using 19 selected indicators.

In order to avoid information overlapping from high-dimensional datasets, dimension reduction is usually performed to get a minimum dataset. Principal component analysis (PCA) is regarded as a statistical procedure using dimension reduction to convert a set of observations with possibly correlated variables into a set of linearly uncorrelated variables called principal components (Liu et al., 2003).

The objectives of this work were: (i) to clarify how 19 selected soil fertility indicators are affected by the succession of rocky desertification, and (ii) to identify some reasonable and sensitive indicators to evaluate soil fertility of karst lands with different RD grades.

2 Materials and methods

2.1 Study area

The sampling sites are in karst region involving five counties, namely Lianyuan (LY), Longhui (LH), Shaodong (SD), Xinhua (XH), and Xinshao (XS), approximately ranging 26°55′–28°18′ N and 110°40′–112°05′ E in the central Hunan province, China. Topographic features of this region include karst landforms and fluvial erosion landforms, characterized by hills, syncline valleys and mountains. The region is a subtropical warm-moist climate with mean annual air temperature of 18.3 °C, and with mean annual precipitations of 1425 mm from 2000 to 2012, which were obtained from China Meteorological Data Sharing Service System online (http://cdc.cma.gov.cn/home.do).

2.2 Soil sampling and handling

We used core cutter (5 cm i.d.) to take the soil samples before covering the holes carefully in the field. There were no endangered or protected species involved in this study. The permissions for sampling locations were approved by Forestry Bureau of Lianyuan (LY), Longhui (LH), Shaodong (SD), Xinhua (XH), and Xinshao (XS) counties, respectively.

Rocky desertification (RD) regions are divided into 4 grades, namely potential RD (PRD), light RD (LRD), moderate RD (MRD), and intensive RD (IRD) based on the soil depth, vegetation coverage, bedrock exposure and vegetation type (Table 1). From 15 to 22 December 2011, four typical plots with different RD grades every county were selected as the sampling sites, which guided by the officials at local Forestry Bureau. The plots, designated LY1–LY4, LH1–LH4, SD1–SD4, XH1–XH4, and XS1–XS4 (Table 1), were all approximately 400 m^2 in area. At each sampling plot, six points were evenly distributed by walking on the way like letter "S" over the area. And at each point, three cores (5 cm diameter, 0–20 cm depth) were taken from three vertices of one triangle patch (0.5 m side length). After plant debris, roots and stones were removed, these three cores were mixed thoroughly in a clean pail without sieving to give one composite sample. Thus, totally 120 soil samples were collected in the field work. Every composite sample was divided into two parts, a field-moist sample and an air-dried one. The field-moist samples were kept in refrigerator under −20 °C until culturing microbe to enumerate bacteria, fungi and actinomycetes, and analyzing microbial biomass carbon (MBC), microbial biomass nitrogen (MBN) and microbial biomass phosphorus (MBP). The air-dried samples were used to determinate chemical and physical parameters.

2.3 Soil physicochemical properties analyses

Soil pH was determined using a combined glass electrode with 1 : 2.5 (w : v) ratios of soil to 1 mol L^{-1} KCl in distilled water. Bulk density (BD), capillary moisture capacity (CMC), field moisture capacity (FMC), capillary porosity (CAP), and total porosity (TOP) were determined by core cutter method. Vegetation coverage was measured on site using digital camera method after calculating the ratio of red to near-infrared brightness of image recorded and processed (Hu et al., 2007; White et al., 2000). Based on calculating the ratio of bedrock area to whole image (Hu et al., 2007; White et al., 2000), bedrock exposure was estimated using dimension measurements on site using a Nikon DTM322 total station surveying instrument (Nikon-Trimble Co. Ltd., Japan). Cation exchange capacity (CEC) was determined by mixed ammonium acetate EDTA method (Zou et al., 2009).

Total organic carbon (TOC) content was measured by dichromate oxidation method (Yeomans and Bremner, 1988). Total nitrogen (TN) was measured by Kjedahl determination method after digestion (Brookes et al., 1985a). Total phosphorus (TP) and total potassium (TK) contents were measured after fusion-pretreated with sodium hydroxide (Smith and Bain, 1982) respectively. Available phosphorus (AP) and available potassium (AK) were tested using Mehlich 3 extracting method (Sims, 1989).

2.4 Soil microbial biomass properties analyses

Measurements of MBC, MBN, and MBP were tested by chloroform-fumigation method (Brookes et al., 1985b; Wu et al., 1990). The density of soil microorganisms including bacteria (BAC), fungi (FUN), and actinomycetes (ACT) were measured by dilution plating method (Bulluck Iii et al., 2002).

2.5 Statistical analyses

The studied variables were analyzed by descriptive statistics (i.e., average of 6 samples in each plot, average within the same desertification level, standard-deviation, correlation coefficient, and principal component analysis). The mean values were compared using Student's *t* test for paired differences at 5 and 1 % level of significance after one-way analysis of variance (ANOVA) are conducted to test homogeneity of variance (*F* test) of 4 RD classes. If the ANOVA *F* test is not significant, no follow-up *t* tests should be used. All statistical analyses were performed using SPSS Statistics (ver. 20, IBM, USA).

2.6 Procedure for evaluating soil fertility using PCA

2.6.1 Standardization of original variables and computation of correlation matrix

Data should be standardized to avoid unexpected influence appearing (Liu et al., 2003) because some of 19 selected indicators are on very different scales. Data standardization can be done facilely in SPSS, which using the equation: $x'_{ij} = (x_{ij} - \overline{x}_i)/S_i$, where x'_{ij} is the standardized value for each indicator; x_{ij} is the original value for each indicator; $\overline{x}_i$ is the mean of original value for each indicator; S_i is the standard deviation for each indicator; $i = 1, 2, \ldots, m$ (number of indicators), herein $m = 19$; and

$j = 1, 2, \ldots, n$ (number of samples), herein $n = 20$. Then, the standardized means of 19 indicators for 20 plots were used to compute the correlation matrix.

2.6.2 Identification of principal components

Principal component is a linear combination of all original indicators, and their loading coefficients are also named characteristic vectors. Although the number of principal components is equal to that of indicators, unlikely the original indicators (some dependent indicators maybe exist), all principal components are not correlated to each other. Generally, first several principal components can represent major information of the samples. Selecting rule for principal components was: (a) eigenvalue of each principal component is bigger than 1; and (b) cumulative variance proportion of all principal components is more than 85 %.

2.6.3 Calculation of principal component scores

Principal component scores of all samples were obtained using the equation: $\boldsymbol{P}_{kj} = \sum_{i=1}^{m} \boldsymbol{A}_{ki} \times x'_{ij}$, where $\boldsymbol{A}_{ki}$ is the characteristic vector based on standardized data matrix; x'_{ij} is the standardized value of evaluating indicators; $k = 1, 2, \ldots, p$ (number of selected principal components according to the rule above); $i = 1, 2, \ldots, m$ (number of indicators); and $j = 1, 2, \ldots, n$ (number of samples).

2.6.4 Calculation of integrated fertility scores

Integrated soil fertility scores were calculated using the equation: $F_j = \sum_{k=1}^{p} \boldsymbol{VAR}_k \times \boldsymbol{P}_{kj}$, where $\boldsymbol{VAR}_k$ is the variance contribution rate for each principal component, i.e. the percentage of the variance for each principal component in the sum of all variances, which means the proportion of information out of the whole sample information deriving from original indicators to each principal component; $\boldsymbol{P}_{kj}$ is the principal component score; $k = 1, 2, \ldots, p$ (number of principal components); and $j = 1, 2, \ldots, n$ (number of samples).

3 Results

3.1 Variation of soil fertility indicators with succession of RD

Using one-way ANOVA, statistical comparison among the measured indicators was performed. The results indicated that the succession of RD affected 19 selected soil fertility indicators to different extent (Table 2). The content of TOC, TN, MBC, MBN, TP, and AP decreased with the aggravation of RD ($p < 0.05$). TOC, TN, MBC, and MBN values for PRD were significantly different from those for LRD, MRD, and IRD, while the difference between those values for LRD and MRD was not significant. There were significant difference between TP of PRD with that of IRD, between AP of PRD with that of LRD or IRD, and between AK of PRD and that of IRD. The changing trend of MBP, BAC, and ACT was: PRD > MRD > LRD > IRD. There were significant difference between MBP for MRD and those for PRD, LRD, and IRD. The changing trend of BD was: IRD > LRD > MRD > PRD without obvious difference. Contrarily, the content of TK, CEC, pH, FUN, CMC, FMC, CAP, and TOP were not significantly different from succession of RD.

3.2 Evaluation of soil fertility using PCA

The correlation matrix for 19 indicators were calculated with the standardized means of 20 plots using SPSS (Table 3). TOC, TN, and TP showed significant and positive correlation with each other, and TOC highly correlated to TN with $r = 0.936$. MBC, MBN, and MBP also significantly and positively correlated to each other. Both CMC and FMC were correlated to TP, AP, TK, CEC, and BD. However, pH, AK, BAC, FUN, and ACT nearly showed no correlation with other indicators. It was notable that the correlation coefficient of BD vs. TOP is −1000 because the TOP was calculated from BD data. Thus, we could remove TOP and TN from dataset of measurements in future study.

PCA was performed using the data matrix of standardized means for 19 indicators. Although there were several highly dependent indicators, all original indicators were grouped into 19 independent principal components. Each eigenvalue of first 6 principal components (PC_1–PC_6) was bigger than 1, and their cumulative variance proportion was 83.8 %, a litter less than 85 % (Table 4). Taken altogether, first 6 principal components could represent the total information of original variables.

The order by which the principal components are interpreted depends on the magnitude of their eigenvalues. The PC_1 explained 31.1 % of the variance (Table 4). It had highly positive loadings from CMC (0.838), FMC (0.821), TN (0.779), CEC (0.766) and TOP (0.746). In a rough sense, the PC_1 was identified as the “*water/air permeability and water-holding capacity component*” since it mainly covered features related to water and air permeability *water-holding capacity* of soil. The PC_2 explained 19.0 % of the variance with highly positive loadings from AP (0.743), MBC (0.679), TOC (0.610), and MBP (0.574). We named PC_2 “*organic matter component*” because all these indicators were significantly correlated to TOC (Table 3).

The PC_3 was defined as the “*microbial biomass component*” because it explained 10.9 % of the variance with positive loadings from MBP (0.592), ACT (0.515), CAP (0.512) and MBN (0.508). Explaining 9.0 % of the variance, the PC_4 was called as “*microbial communities component*” because it had positive loading from FUN (0.593).

The PC_5 explained 8.4 % of the variance and was defined as the “*phosphorus nutrient component*” because it had positive loading from TP (0.572). The PC_6 explained 5.4 % of the variance and was referred to “*potassium nutrient component*” since it had positive loading from AK (0.613).

After computing principal component scores, integrated soil fertility scores of 20 plots were calculated (Fig. 1). Fertility level of sampling sites LY1 and XH1 for PRD was higher than those of other sites as expected, but fertility scores of LH1 and XS1 for

PRD were lower than fertility scores of LH2 and LY2 for LRD, and fertility scores of LH3, XH3 and XS3 for MRD. Fertility scores of LY4 and SD4 for IRD were far lower than those of other sites. In summary, integrated fertility scores fluctuated with different sampling sites for different RD grades.

To facilitate comparison, the means of integrated fertility scores were calculated (Fig. 2). The sequencing of the mean scores was PRD > MRD > LRD > IRD. The difference between fertility scores of PRD and those of IRD was very significant ($p = 0.008$), and the difference between fertility scores of LRD and those of IRD was significant ($p = 0.023$). However, fertility scores of PRD vs. LRD ($p = 0.622$), PRD vs. MRD ($p = 0.160$), LRD vs. MRD ($p = 0.692$), and MRD vs. IRD ($p = 0.416$) were not significantly different.

3.3 Correlation of integrated fertility scores with evaluating indicators

We analyzed the correlation of integrated soil fertility scores with the 19 evaluating indicators (Table 5). The results demonstrated that the integrated fertility scores were strongly and significantly correlated to TOC, TN, TP, CEC, MBC, MBN, MBP and BD ($p < 0.01$), were significantly correlated to TK, AK, FUN, FMC, and TOP, but were insignificantly correlated to pH, AP, BAC, ACT, CMC, and CAP.

4 Discussions

4.1 Effects of succession of RD on soil fertility

Soil fertility, as the basis of soil quality, directly affects the productivity of land. In return, land use type and frequency influence the soil quality (Ozgoz et al., 2013). The aggravation of RD is not only caused by anthropogenic factor (land overuse), but also by climate (S. Li et al., 2009). Degradation of phytocommunity (tree → tree/shrub → shrub → shrub/grass → grass) results in homogenized community structure, decrease of biomass and litter fall, and reduction of plant nutrition such as soil organic matter, total N and so on. The altered soil ecosystem leads to microorganism population reducing and microbial degradation of litter fall decreasing, so that C, N, and P retentions in soil decrease (Lu et al., 2014). First two components (Table 4) were identified as "*water/air permeability and water-holding capacity component*" and "*organic matter component*", so water/air permeability, water-holding capacity, and organic matter content would be affected strongly by the aggravation of RD. Thus, the aggravation of RD leads to soil hardening, bulk density enlarging, water/air permeability worsening, and water-holding ability of surface soil decreasing would happen, then the strong surface runoff causes great loss of N, P, and K nutrients (Peng and Wang, 2012). In one word, multiple affects above eventually lead to integrated soil fertility decreasing with the aggravation of RD.

4.2 Discordance between soil fertility level and RD grade

Soil fertility fluctuated remarkably with different sampling sites and with different RD grades. Soil fertility levels were not always consistent with RD grades, for instance, the average fertility of MRD was greater than that of LRD (Fig. 2). This might be ascribed to: (i) the classification method of RD is not so satisfactory as expected. The actual soil fertility could not be only explored from soil depth, vegetation coverage, bedrock exposure and vegetation type. For some karst areas (MRD or IRD), although their vegetation covers are less than those of LRD, their surface fertile soil might accumulate in a low-lying zone when eroded by rainfall chronically, hence some soil with higher RD grade would have greater fertility, (ii) difference of soil fertility also caused by regional variation. Local climate, soil-forming conditions, and the way and extent of anthropogenic intervention were different from one region to another (Clemens et al., 2010). Soil fertility in one region for MRD might be greater than that in another region for LRD. When we investigated on stands, we found that the majority of PRD regions had better vegetation because they had been enclosed for afforestation to avoid anthropogenic interference. Most of IRD regions became abandoned land without any agricultural production due to seriously degrading soil fertility. In contrast, both LRD and MRD regions with moderate fertility were not strictly protected. Perhaps residue burning had caused degradation of tree/shrub to shrub/grass or animal grazing had led to residue mineralization, recycling of faeces, and incrementing soil nutrients. They were usually utilized to cultivate timber forests or non-wood forests. As a result, the anthropogenic interference to LRD or MRD certainly reached the highest level. Human activity is one of key driving factors of RD (Y. B. Li et al., 2009; Xiong et al., 2009), and RD grade varies among land use types (Li et al., 2006). Thus, reducing human activities and taking measurements such as mountain closure, forest reservation and plantation might be definitely important to control expanding of RD area, which could be learned from natural vegetation rehabilitation to control soil erosion on the Loess Plateau (G. Zhao et al., 2013a; X. Zhao et al., 2013), (iii) self-organization of soil environment improves soil fertility. With gradual deterioration of soil fertility, soil animals and microorganism at some stage (MRD) increase the speed of litter fall breakdown by disintegrating tissue and fixing the nutrients to acclimate the degrading environment (Barot et al., 2007). Thus, the fertility of MRD soil is likely greater than that of LRD soil.

4.3 Sensitive indicators to evaluate soil fertility in RD lands

Selecting appropriate indicators will guarantee the accuracy of evaluating results. Generally, evaluating indicators are chosen empirically based on the researching fruits of predecessors. Some physiochemical (Ozgoz et al., 2013), microbial biomass (Paz-Ferreiro and Fu, 2013), and enzymatic activity properties (Pajares et al., 2011) had been chosen to assess the soil quality. On the basis of scientifically reliability, defining a minimum dataset for evaluating soil fertility can cut down the number of indicators and reduce evaluating cost.

Soil organic matter (used interchangeably with TOC), as the major source of several nutrients, exerts numerous positive effects on soil physiochemical properties, as well as soil's capacity to provide regulatory ecosystem services. N, P, and K are often referred to the primary macronutrients in soil for plants' growth. CEC is used as a measure of fertility and nutrient retention capacity. BD, as an indicator of soil compaction, reflects the loosen extent and permeability of soil. MBC, MBN, and MBP, reflects the number and activity of soil microorganism, and the status of soil environment, although they only have a little content in soil with the mean ratios of MBC to TOC (0.61 %), MBN to TN (2.16 %), and MBP to TP (0.95 %) in this study (extracting from Table 2). It was reported that the microbial activity directly influences soil ecosystem stability and fertility (Pascual et al., 1997). Soil biochemical, microbiological and biological properties are more suitable than physical and/or chemical properties to estimate soil quality and soil degradation (Paz-Ferreiro and Fu, 2013). And it is widely recognized that a good level of microbiological activity is crucial for maintaining soil quality (de la Paz Jimenez et al., 2002; Pascual et al., 2000; Visser and Parkinson, 1992), because microbial turnover is a driving force for transformation and cycling of organic matter to plant nutrients in soils (Chen and He, 2002; Fontaine et al., 2003). For instance, the changes in MBC is a sensitive index of changes in the content of soil organic matter (García-Orenes et al., 2010; Powlson et al., 1987), and it is useful for determining microbial population size to evaluate natural and degraded systems (Soulas et al., 1984). The strong and positive correlation between MBC and TOC (Table 3) indicated that MBC was a sensitive index to indicate the dynamics of soil organic carbon (Liu et al., 2012). Inorganic N and P needed by vegetation are mainly obtained from mineralization of organic matter in soil microbial degradation system (Hopkins et al., 2011; Ros et al., 2011). The changes in MBN and MBP can also indicate the fluctuation of soil fertility (Powlson et al., 1987). Thus, these indicators deserve pre-researching before getting a minimum dataset.

Furthermore, TOC, TN, TP, CEC, MBC, MBN, MBP, and BD were strongly and significantly correlated to the integrated soil fertility ($p < 0.01$) (Table 5). But TN was highly correlated to TOC with $r = 0.936$ (Table 3). Thus, we can put forward that TOC, TP, CEC, MBC, MBN, MBP, and BD might be reasonable and sensitive indicators to estimate soil fertility in RD region. They could be included in the minimum dataset of evaluating indicators for RD.

5 Conclusions

The succession of RD affected evaluating indicators of soil fertility to different extent, but the degradation trend of soil fertility was almost parallel to the aggravation of RD. Soil chemical indicators TOC, TP and CEC, microbial indicators MBC, MBN and MBP, and physical indicator BD might be the key indicators to evaluate soil fertility in RD regions according to their paired correlations and significant correlation to the integrated soil fertility. Perhaps the method of classifying RD only according to soil depth and the landscape indicators (vegetation coverage, bedrock exposure, and vegetation type) could be improved after taking the regional difference of soil fertility into account in the future research.

Acknowledgements. This research was supported by National Department Public Benefit Research Foundation of State Forestry Administration of China (201104016) and the Planned Science and Technology Project of Hunan Province, China (2013RS4035), and was partially funded by the China Postdoctoral Science Foundation (2013M531787). We thank Veronika for her critical revision of the manuscript. We are grateful to the Forestry Bureau of Lianyuan, Longhui, Shaodong, Xinhua, and Xinshao counties of Hunan for providing the sampling sites. We also acknowledge the anonymous reviewers for the valuable comments.

References

Bai, X. Y., Wang, S. J., and Xiong, K. N.: Assessing spatial–temporal evolution processes of karst rocky desertification land: Indications for restoration strategies, Land Degrad. Dev., 24, 47–56, 2013.

Barot, S., Rossi, J. P., and Lavelle, P.: Self-organization in a simple consumer-resource system, the example of earthworms, Soil Biol. Biochem., 39, 2230–2240, 2007.

Brookes, P. C., Kragt, J. F., Powlson, D. S., and Jenkinson, D. S.: Chloroform fumigation and the release of soil nitrogen: the effects of fumigation time and temperature, Soil Biol. Biochem., 17, 831–835, 1985a.

Brookes, P. C., Landman, A., Pruden, G., and Jenkinson, D. S.: Chloroform fumigation and the release of soil nitrogen: a rapid direct extraction method to measure microbial biomass nitrogen in soil, Soil Biol. Biochem., 17, 837–842, 1985b.

Bulluck Iii, L. R., Brosius, M., Evanylo, G. K., and Ristaino, J. B.: Organic and synthetic fertility amendments influence soil microbial, physical and chemical properties on organic and conventional farms, Appl. Soil Ecol., 19, 147–160, 2002.

Cerdà, A. and Lavée, H.: The effect of grazing on soil and water losses under arid and Mediterranean climates. Implications for desertification, Pirineos, 153, 159–174, 1999.

Chen, G. C. and He, Z. L.: Microbial biomass phosphorus turnover in variable-charge soils in China, Commun. Soil Sci. Plan., 33, 2101–2117, 2002.

Clemens, G., Fiedler, S., Cong, N. D., Van Dung, N., Schuler, U., and Stahr, K.: Soil fertility affected by land use history, relief position, and parent material under a tropical climate in NW-Vietnam, Catena, 81, 87–96, 2010.

de la Paz Jimenez, M., de la Horra, A., Pruzzo, L., and Palma, M.: Soil quality: a new index based on microbiological and biochemical parameters, Biol. Fert. Soils, 35, 302–306, 2002.

Deng, Y. and Jiang, Z. C.: Characteristic of rocky desertification and comprehensive improving model in karst peak-cluster depression in Guohua, Guangxi, China, Procedia Environmental Sciences, 10, 2449–2452, 2011.

Fallahzade, J. and Hajabbasi, M. A.: The effects of irrigation and cultivation on the quality of desert soil in central Iran, Land Degrad. Dev., 23, 53–61, 2012.

Fontaine, S., Mariotti, A., and Abbadie, L.: The priming effect of organic matter: a question of microbial competition?, Soil Biol. Biochem., 35, 837–843, 2003.

Fu, B., Li, S., Yu, X., Yang, P., Yu, G., Feng, R., and Zhuang, X.: Chinese ecosystem research network: progress and perspectives, Ecol. Complex., 7, 225–233, 2010.

García-Orenes, F., Guerrero, C., Roldán, A., Mataix-Solera, J., Cerdà, A., Campoy, M., Zornoza, R., Bárcenas, G., and Caravaca, F.: Soil microbial biomass and activity under different agricultural management systems in a semiarid Mediterranean agroecosystem, Soil Till. Res., 109, 110–115, 2010.

Hopkins, D. W., Waite, I. S., and O'Donnell, A. G.: Microbial biomass, organic matter mineralization and nitrogen in soils from long-term experimental grassland plots (Palace Leas meadow hay plots, UK), Eur. J. Soil Sci., 62, 95–104, 2011.

Hu, Z. Q., He, F. Q., Yin, J. Z., Lu, X., Tang, S. L., Wang, L. L., and Li, X. J.: Estimation of fractional vegetation cover based on digital camera survey data and a remote sensing model, Journal of China University of Mining and Technology, 17, 116–120, 2007.

Huang, Q. H. and Cai, Y. L.: Spatial pattern of karst rock desertification in the middle of Guizhou province, southwestern China, Environ. Geol., 52, 1325–1330, 2007.

Huang, Q. H., Cai, Y. L., and Xing, X. S.: Rocky desertification, antidesertification, and sustainable development in the karst mountain region of southwest China, Ambio, 37, 390–392, 2008.

Li, C., Xiong, K., and Wu, G.: Process of biodiversity research of Karst areas in China, Acta Ecologica Sinica, 33, 192–200, 2013.

Li, S., Wei, X., Huang, J., Wang, X., Lu, G., and Li, H.: The causes and processes responsible for rocky desertification in karst areas of southern China, Sciences in Cold and Arid Regions, 1, 0080–0090, 2009.

Li, Y. B., Bai, X. Y., and Qiu, X. C.: The correlation analysis of desertification of karst rock and land use patterns, Resources Science, 28, 68–73, 2006 (in Chinese with English abstract).

Li, Y. B., Shao, J. A., Yang, H., and Bai, X. Y.: The relations between land use and karst rocky desertification in a typical karst area, China, Environ. Geol., 57, 621–627, 2009.

Liu, N., Zhang, Y., Chang, S., Kan, H., and Lin, L.: Impact of grazing on soil carbon and microbial biomass in typical steppe and desert steppe of Inner Mongolia, PLoS ONE, 7, e36434, doi:10.1371/journal.pone.0036434, 2012.

Liu, R. X., Kuang, J., Gong, Q., and Hou, X. L.: Principal component regression analysis with SPSS, Comput. Meth. Prog. Bio., 71, 141–147, 2003.

Liu, Z.-F., Fu, B.-J., Liu, G.-H., and Zhu, Y.-G.: Soil quality: concept, indicators and its assessment, Acta Ecologica Sinica, 26, 901–913, 2006 (in Chinese with English abstract).

Lu, X., Toda, H., Ding, F., Fang, S., Yang, W., and Xu, H.: Effect of vegetation types on chemical and biological properties of soils of karst ecosystems, Eur. J. Soil Biol., 61, 49–57, 2014.

Ozgoz, E., Gunal, H., Acir, N., Gokmen, F., Birol, M., and Budak, M.: Soil quality and spatial variability assessment of land use effects in a tipic Haplustoll, Land Degrad. Dev., 24, 277–286, 2013.

Pajares, S., Gallardo, J. F., Masciandaro, G., Ceccanti, B., and Etchevers, J. D.: Enzyme activity as an indicator of soil quality changes in degraded cultivated Acrisols in the Mexican Trans-volcanic Belt, Land Degrad. Dev., 22, 373–381, 2011.

Pascual, J. A., García, C., Hernandez, T., and Ayuso, M.: Changes in the microbial activity of an arid soil amended with urban organic wastes, Biol. Fert. Soils, 24, 429–434, 1997.

Pascual, J. A., Garcia, C., Hernandez, T., Moreno, J. L., and Ros, M.: Soil microbial activity as a biomarker of degradation and remediation processes, Soil Biol. Biochem., 32, 1877–1883, 2000.

Paz-Ferreiro, J. and Fu, S.: Biological indices for soil quality evaluation: perspectives and limitations, Land Degrad. Dev., doi:10.1002/ldr.2262, online first, 2013.

Peng, T. and Wang, S.-J.: Effects of land use, land cover and rainfall regimes on the surface runoff and soil loss on karst slopes in southwest China, Catena, 90, 53–62, 2012.

Powlson, D. S., Prookes, P. C., and Christensen, B. T.: Measurement of soil microbial biomass provides an early indication of changes in total soil organic matter due to straw incorporation, Soil Biol. Biochem., 19, 159–164, 1987.

Ros, G. H., Temminghoff, E. J. M., and Hoffland, E.: Nitrogen mineralization: a review and meta-analysis of the predictive value of soil tests, Eur. J. Soil Sci., 62, 162–173, 2011.

Sims, J.: Comparison of mehlich 1 and mehlich 3 extractants for P, K, Ca, Mg, Mn, Cu and Zn in atlantic coastal plain soils, Commun. Soil Sci. Plan., 20, 1707–1726, 1989.

Smith, B. F. L. and Bain, D. C.: A sodium hydroxide fusion method for the determination of total phosphate in soils, Commun. Soil Sci. Plan., 13, 185–190, 1982.

Soulas, G., Chaussod, R., and Verguet, A.: Chloroform fumigation technique as a means of determining the size of specialized soil microbial populations: application to pesticide-degrading microorganisms, Soil Biol. Biochem., 16, 497–501, 1984.

Tilman, D., Cassman, K. G., Matson, P. A., Naylor, R., and Polasky, S.: Agricultural sustainability and intensive production practices, Nature, 418, 671–677, 2002.

Visser, S. and Parkinson, D.: Soil biological criteria as indicators of soil quality: soil microorganisms, Am. J. Alternative Agr., 7, 33–37, 1992.

Wang, H. and Jia, X.: Field observations of windblown sand and dust in the Takimakan Desert, NW China, and insights into modern dust sources, Land Degrad. Dev., 24, 323–333, 2013.

Wang, S. and Li, Y.: Problems and development trends about researches on karst rocky desertification, Advances in Earth Science, 22, 573–582, 2007 (in Chinese with English abstract).

Wang, S. J., Li, R. L., Sun, C. X., Zhang, D. F., Li, F. Q., Zhou, D. Q., Xiong, K. N., and Zhou, Z. F.: How types of carbonate rock assemblages constrain the distribution of karst rocky desertified land in Guizhou Province, PR China: phenomena and mechanisms, Land Degrad. Dev., 15, 123–131, 2004a.

Wang, S. J., Liu, Q. M., and Zhang, D. F.: Karst rocky desertification in southwestern China: geomorphology, landuse, impact and rehabilitation, Land Degrad. Dev., 15, 115–121, 2004b.

Wang, T., Yan, C. Z., Song, X., and Li, S.: Landsat images reveal trends in the aeolian desertification in a source area for sand and dust storms in China's Alashan Plateau (1975–2007), Land Degrad. Dev., 24, 422–429, 2013.

Wang, X., Wang, G., Lang, L., Hua, T., and Wang, H.: Aeolian transport and sandy desertification in semiarid China: a wind tunnel approach, Land Degrad. Dev., 24, 605–612, 2013.

White, M. A., Asner, G. P., Nemani, R. R., Privette, J. L., and Running, S. W.: Measuring fractional cover and leaf area index in arid ecosystems: digital camera, radiation transmittance, and laser altimetry methods, Remote Sens. Environ., 74, 45–57, 2000.

Wu, J., Joergensen, R. G., Pommerening, B., Chaussod, R., and Brookes, P. C.: Measurement of soil microbial biomass C by fumigation-extraction-an automated procedure, Soil Biol. Biochem., 22, 1167–1169, 1990.

Wu, X. Q., Liu, H. M., Huang, X. L., and Zhou, T.: Human driving forces: analysis of rocky desertification in karst region in Guanling County, Guizhou Province, Chinese Geographical Science, 21, 600–608, 2011.

Xie, L. and Wang, S.: Variations of nutrient element contents of plants and soils in the process of karst rocky desertification, Chinese Journal of Geochemistry, 25, p. 176, 2006.

Xiong, Y. J., Qiu, G. Y., Mo, D. K., Lin, H., Sun, H., Wang, Q. X., Zhao, S. H., and Yin, J.: Rocky desertification and its causes in karst areas: a case study in Yongshun County, Hunan Province, China, Environ. Geol., 57, 1481–1488, 2009.

Yan, X. and Cai, Y. L.: Multi-scale anthropogenic driving forces of karst rocky desertification in southwest China, Land Degrad. Dev., doi:10.1002/ldr.2209, online first, 2013.

Yao, R., Yang, J., Gao, P., Zhang, J., and Jin, W.: Determining minimum data set for soil quality assessment of typical salt-affected farmland in the coastal reclamation area, Soil Till. Res., 128, 137–148, 2013.

Yeomans, J. C. and Bremner, J. M.: A rapid and precise method for routine determination of organic carbon in soil, Commun. Soil Sci. Plan., 19, 1467–1476, 1988.

Zhao, G., Mu, X., Wen, Z., Wang, F., and Gao, P.: Soil erosion, conservation, and eco-environment changes in the Loess plateau of China, Land Degrad. Dev., 24, 499–510, 2013.

Zhao, X., Wu, P., Gao, X., and Persaud, N.: Soil quality indicators in relation to land use and topography in a small catchment on the Loess Plateau of China, Land Degrad. Dev., doi:10.1002/ldr.2199, online first, 2013.

Zou, Z., Qiu, R., Zhang, W., Dong, H., Zhao, Z., Zhang, T., Wei, X., and Cai, X.: The study of operating variables in soil washing with EDTA, Environ. Pollut., 157, 229–236, 2009.

Table 1. Classification of rocky desertification and basic information of plots.

Grade	Vegetation	Utilization	Soil depth /cm	Vegetation coverage /%	Bedrock exposure /%	Serial no. of plots
PRD	tree	forest conversation	> 40	> 70	< 30	LH1, LY1, SD1, XH1, XS1
LRD	tree, shrub	timber stands, non-wood forests	30–40	50–70	30–39	LH2, LY2, SD2, XH2, XS2
MRD	shrub	non-wood forest, abandoned land	20–29	30–49	40–49	LH3, LY3, SD3, XH3, XS3
IRD	grass	abandoned land	10–19	20–29	50–69	LH4, LY4, SD4, XH4, XS4

PRD, LRD, MRD, and IRD are potential, light, moderate, and intensive rocky desertification respectively.

Table 2. Effects of succession of rocky desertification on soil quality indicators.

Test items	PRD	LRD	MRD	IRD
pH	5.72 ± 1.26a	6.18 ± 1.09a	6.55 ± 0.64a	6.16 ± 0.10a
TOC (g kg^{-1})	27.50 ± 4.30a	25.32 ± 7.97b	19.10 ± 1.42b	16.86 ± 2.99c
TN (g kg^{-1})	2.64 ± 0.40a	2.31 ± 0.87b	1.77 ± 0.15b	1.41 ± 0.41c
TP (g kg^{-1})	0.58 ± 0.05a	0.45 ± 0.21ab	0.39 ± 0.06ab	0.43 ± 0.14b
AP (mg kg^{-1})	1.37 ± 0.49a	1.12 ± 0.90b	0.60 ± 0.45ab	0.19 ± 0.11c
TK (g kg^{-1})	8.67 ± 4.52a	10.90 ± 5.28a	12.33 ± 8.09a	11.83 ± 2.84a
AK (mg kg^{-1})	95.60 ± 22.13a	85.98 ± 31.83ab	89.25 ± 47.34ab	64.51 ± 19.66b
CEC (cmol kg^{-1})	27.12 ± 9.95a	24.87 ± 7.31a	24.02 ± 8.66a	24.72 ± 3.84a
MBC (mg kg^{-1})	230.87 ± 31.03a	160.58 ± 48.73b	103.45 ± 53.51b	43.74 ± 4.56c
MBN (mg kg^{-1})	64.41 ± 27.98a	53.80 ± 18.78b	34.03 ± 4.05b	23.48 ± 2.86c
MBP (mg kg^{-1})	6.95 ± 1.41a	3.34 ± 0.65a	4.22 ± 0.80b	3.07 ± 0.92a
BAC (× 10^3 CFU g^{-1})	1.41 ± 1.57a	0.92 ± 0.97b	1.22 ± 1.39a	0.46 ± 0.17a
FUN (× 10^3 CFU g^{-1})	2.61 ± 2.03a	1.49 ± 1.70a	1.79 ± 1.25b	2.09 ± 2.29a
ACT (× 10^3 CFU g^{-1})	7.37 ± 14.64a	2.05 ± 1.88b	3.30 ± 4.99a	0.44 ± 0.28a
BD (g cm^{-3})	1.26 ± 0.18a	1.33 ± 0.14a	1.29 ± 0.12a	1.39 ± 0.08a
CMC (%)	0.33 ± 0.04a	0.36 ± 0.09a	0.38 ± 0.05a	0.33 ± 0.03a
FMC (g g^{-1})	0.26 ± 0.08a	0.28 ± 0.09a	0.27 ± 0.09a	0.25 ± 0.03a
CAP (%)	0.42 ± 0.09a	0.46 ± 0.06a	0.48 ± 0.04a	0.45 ± 0.02a
TOP (%)	0.52 ± 0.07a	0.50 ± 0.05a	0.51 ± 0.04a	0.48 ± 0.03a

TOC, total organic carbon; TN, total nitrogen; TP, total phosphorus; AP, available phosphorus; TK, total potassium; AK, available potassium; CEC, cation exchange capacity; MBC, microbial biomass carbon; MBN, microbial biomass nitrogen; MBP, microbial mass phosphorous; BAC, bacteria; FUN, fungi; ACT, actinomycetes; BD, bulk density; CMC, capillary moisture capacity; FMC, field moisture capacity; CAP, capillary porosity; TOP, total porosity.

Means ± SD within each column, for each indicator, followed by the same letter are not significantly different in ANOVA *F* test, by least significant difference (LSD) at $p \leq 0.05$.

Table 3. Correlation matrix of soil evaluating indicators for rocky desertification[a].

	pH	TOC	TN	TP	AP	TK	AK	CEC	MBC	MBN	MBP	BAC	FUN	ACT	BD	CMC	FMC	CAP
TOC	−0.158	1																
TN	0.097	0.936[c]	1															
TP	−0.049	0.555[b]	0.678[c]	1														
AP	−0.458[b]	0.308	0.125	−0.065	1													
TK	0.357	0.009	0.116	0.406	−0.476[b]	1												
AK	0.032	−0.036	−0.027	0.095	0.277	0.365	1											
CEC	0.285	0.375	0.514[b]	0.253	−0.335	0.312	0.165	1										
MBC	−0.188	0.678[c]	0.514[b]	0.049	0.255	−0.056	0.046	0.175	1									
MBN	−0.036	0.530[b]	0.536[b]	0.274	−0.037	0.00	−0.052	0.118	0.690[c]	1								
MBP	−0.317	0.217	0.104	−0.055	0.101	−0.224	−0.124	0.085	0.580[c]	0.439	1							
BAC	0.348	0.129	0.254	0.026	−0.113	−0.023	0.005	0.573[c]	0.150	0.242	0.192	1						
FUN	−0.379	−0.314	−0.463[b]	−0.205	−0.001	−0.029	−0.021	−0.361	−0.064	−0.054	0.218	−0.240	1					
ACT	−0.233	0.090	−0.062	−0.032	0.227	−0.106	−0.052	−0.100	0.277	−0.062	0.602[c]	0.059	0.380	1				
BD	0.100	−0.562[c]	−0.548[b]	−0.332	−0.093	−0.233	−0.310	−0.664[c]	−0.314	−0.182	−0.126	−0.432	0.131	0.096	1			
CMC	0.263	0.302	0.448[b]	0.587[c]	−0.455[b]	0.577[c]	0.266	0.534[b]	0.094	0.379	−0.035	0.361	−0.113	−0.061	−0.522[b]	1		
FMC	0.278	0.236	0.404	0.447[b]	−0.641[c]	0.526[b]	0.112	0.664[c]	0.099	0.442	−0.020	0.402	−0.147	−0.282	−0.466[b]	0.861[c]	1	
CAP	0.364	−0.091	0.097	0.421	−0.613[c]	0.474[b]	0.101	0.173	−0.125	0.308	−0.096	0.135	−0.033	−0.011	0.107	0.787[c]	0.681[c]	1
TOP	−0.100	0.562[c]	0.548[b]	0.332	0.093	0.232	0.310	0.664[c]	0.314	0.182	0.126	0.433	−0.131	−0.096	−1.000[c]	0.522[b]	0.466[b]	−0.108

[a] The standardized means of 20 plots were used to compute the correlation matrix.
[b] Significant (two-tailed) at $p \leq 0.05$ level.
[c] Significant (two-tailed) at $p \leq 0.01$ level.

Table 4. Principle components analysis.

Items	Characteristic vector of principal component					
	PC_1–A_1	PC_2–A_2	PC_3–A_3	PC_4–A_4	PC_5–A_5	PC_6–A_6
pH	0.229	−0.590	−0.096	−0.283	−0.369	0.422
TOC	**0.655**	**0.610**	−0.051	−0.302	0.212	−0.039
TN	**0.779**	0.372	−0.090	−0.408	0.151	−0.007
TP	**0.628**	−0.021	0.054	−0.163	**0.572**	−0.134
AP	−0.264	**0.743**	−0.347	0.043	0.238	0.289
TK	0.470	−0.520	0.033	0.261	0.322	0.181
AK	0.216	−0.055	−0.311	**0.520**	0.312	**0.613**
CEC	**0.766**	−0.074	−0.217	0.143	−0.388	−0.071
MBC	0.395	**0.679**	0.318	−0.104	−0.066	0.265
MBN	**0.523**	0.309	**0.508**	−0.314	0.014	0.110
MBP	0.106	**0.574**	**0.592**	0.212	−0.291	0.044
BAC	**0.500**	0.012	−0.036	0.093	−0.688	0.115
FUN	−0.346	0.062	0.446	**0.593**	0.162	−0.271
ACT	−0.133	0.396	**0.515**	0.370	−0.058	0.201
BD	−0.746	−0.298	0.369	−0.380	0.069	0.186
CMC	**0.838**	−0.349	0.205	0.173	0.149	0.003
FMC	**0.821**	−0.407	0.195	0.058	−0.058	−0.171
CAP	0.436	−0.627	**0.512**	−0.044	0.180	0.129
TOP	**0.746**	0.299	−0.369	0.380	−0.070	−0.186
Eigenvalue	5.915	3.598	2.078	1.702	1.601	1.020
Variance contribution rate/%	31.131	18.939	10.938	8.959	8.424	5.370
Cumulative variance proportion/%	31.131	50.070	61.008	69.967	78.391	83.761

Table 5. Correlation analysis of integrated fertility scores (*F*) with soil indicators.

	pH	TOC	TN	TP	AP	TK	AK	CEC	MBC	MBN
F	0.111	0.497[b]	0.571[b]	0.465[b]	−0.105	0.145[a]	0.179[a]	0.764[b]	0.503[b]	0.480[b]
	MBP	BAC	FUN	ACT	BD	CMC	FMC	CAP	TOP	
F	0.445[b]	0.424	−0.295[a]	−0.091	−0.679[b]	0.449	0.528[a]	0.077	0.679[a]	

[a] Significant (two-tailed) at $p \le 0.05$ level.

[b] Significant (two-tailed) at $p \le 0.01$ level.

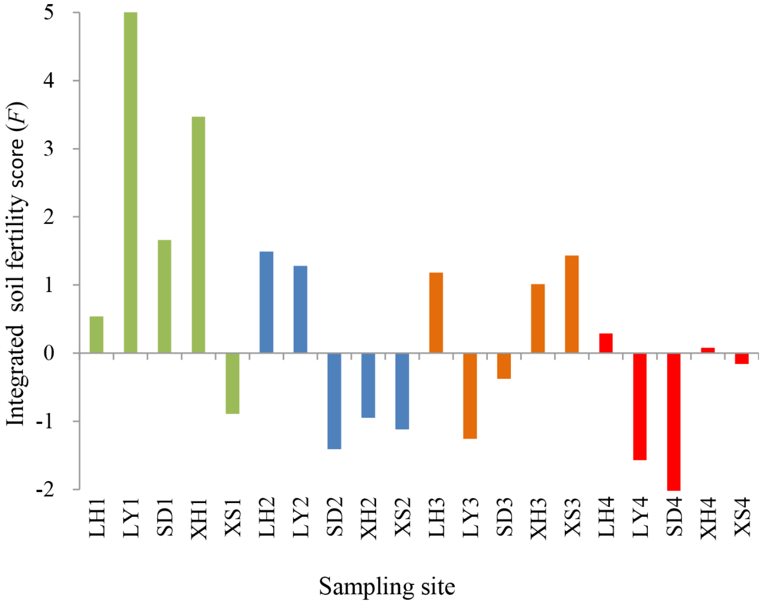

Figure 1. Integrated soil fertility scores of 20 studied plots. LH, LY, SD, XH, and XS are the sampling plots standing for Longhui, Lianyuan, Shaodong, Xinhua, and Xinshao counties at central Hunan province, China, respectively. The green, blue, orange, and red bar refer to potential, light, moderate, and intensive rocky desertification, respectively.

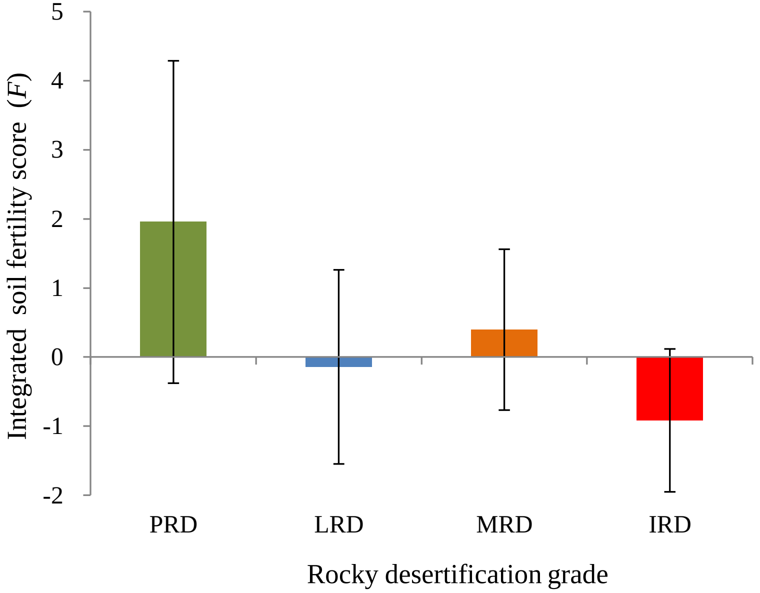

Figure 2. Average scores of integrated soil fertility of 20 studied plots. PRD, LRD, MRD, and IRD refer to potential, light, moderate, and intensive rocky desertification, respectively. Paired difference were analyzed as p (LRD) = 0.114, p (MRD) = 0.347, and p (IRD) = 0.120 compared to PRD.